Journal of
Molluscan Studies

The Malacological Society of London

Journal of Molluscan Studies (2019) **00**: 1–14. doi:10.1093/mollus/eyz032

High genetic connectivity in a gastropod with long-lived planktonic larvae

Fabio Crocetta[1], Luigi Caputi[1], Sofia Paz-Sedano[1], Valentina Tanduo[1,2], Angelo Vazzana[3] and Marco Oliverio[4]

[1] *Department of Integrative Marine Ecology, Stazione Zoologica Anton Dohrn, Villa Comunale, I-80121 Napoli, Italy;*
[2] *Department of Biology, University of Padova, Via U. Bassi 58/B, I-35131 Padova, Italy;*
[3] *Museo di Biologia Marina e Paleontologia di Reggio Calabria, Via Stradella Giuffrè I 32 I-89122 Reggio Calabria, Italy; and*
[4] *Dipartimento di Biologia e Biotecnologie 'Charles Darwin', Università di Roma 'La Sapienza', Viale dell'Università 32, I-00185, Rome, Italy.*

Correspondence: F. Crocetta; e-mail: fabio.crocetta@szn.it

(Received 30 June 2019; editorial decision 7 August 2019)

ABSTRACT

Genetic connectivity plays a crucial role in shaping the geographic structure of species. Our aim in this study was to explore the pattern of genetic connectivity in *Bursa scrobilator*, an iconic marine caenogastropod with long-lived pelagic larvae. Our study was based on the analysis of DNA sequence data for the 658-bp barcoding fragment of the mitochondrial cytochrome *c* oxidase subunit I (COI) gene. This is the largest DNA sequence dataset assembled to date for *B. scrobilator*. These data confirm that the two recently described subspecies *B. scrobilator scrobilator* (Linnaeus, 1758), from the Mediterranean and Macaronesia, and *B. s. coriacea* (Reeve, 1844), from West Africa, constitute two evolutionarily significant units (ESUs). We found that for the nominal subspecies, the variation in morphology (shell, radula and gross anatomy) and DNA sequences was not geographically structured, and this agrees with what we would expect in a species with high connectivity at the larval stage. The divergence between the two subspecies cannot be easily explained by isolation by distance, and we would argue that one or more extrinsic factors may have played a role in isolating the two ESUs and maintaining that isolation.

INTRODUCTION

Connectivity among populations of marine invertebrates is known to have remarkable short-to-medium term effects on genetic variability, genetic structure, range dynamics and persistence, as well as long-term effects on speciation patterns (Lowe & Allendorf, 2010; Castelin *et al.*, 2012 and references therein). For these reasons, connectivity is considered to be a key factor affecting the resilience of species to global change (Mawdsley *et al.*, 2009). In benthic invertebrates, population connectivity is primarily related to dispersal, which tends to occur mostly in the earliest life history stages, the adult stage being only slightly mobile or, in some cases, even sessile (Knowlton & Jackson, 1993; Cowen & Sponaugle, 2009; Ellingson & Krug, 2016). The duration of the pelagic larval phase (PLD), that is, the length of time that a larva spends in the water column before settling, is one of the major factors affecting connectivity. Other influential factors (both intrinsic and extrinsic) include habitat characteristics, currents and larval life history traits, such as mortality and settlement competency features. The correlation between PLD and the level of genetic structure has been shown by many studies (Modica *et al.*, 2017 and references therein). However, the adequacy of PLD as a predictor of genetic connectivity has been questioned by a few workers (e.g. Shanks, 2009); other factors such as habitat differences (Ayre *et al.*, 2009) and past biogeographical events (Edmands, 2001; Marko, 2004) may have had a substantial impact on connectivity.

In marine gastropods, development may either be entirely intracapsular or may include a pelagic phase, during which larvae actively feed on plankton (planktotrophy) or only rely on yolk reserves (lecithotrophy) (Thorson, 1950). Marine gastropods are thus excellent models for testing the influence of PLD and dispersal capacity on genetic structure. An additional advantage is that the developmental type can often be inferred from the morphology of the protoconch, the embryonic and larval shell (i.e. shell developed before metamorphosis or before hatchlings emerge from eggs) that constitutes the initial whorls of the adult shell (Jablonski & Lutz, 1983; Lima & Lutz, 1990). Among gastropods, the *Tonnoidea* (frog shells, tun shells and trumpet shells; Beu, 1997, 1998) are particularly interesting because some species have a long planktonic larval stage (teleplanic larvae) that extends up to several years (e.g. Strathmann & Strathmann, 2007). Only recently has the molecular systematics of the family *Bursidae* begun to be investigated (Castelin *et al.*, 2012; Sanders *et al.*, 2017; Strong *et al.*, 2019); the same holds true for *Bursa scrobilator* (Linnaeus, 1758), one of the most iconic marine gastropods of the Eastern Atlantic and Mediterranean. On the basis of extensive shell-based studies and a molecular phyloge-

netic analysis of some Mediterranean and Senegalese specimens, Smriglio *et al.* (2019) proposed that *B. scrobilator* consists of two subspecies: *B. scrobilator scrobilator* (Linnaeus, 1758) and *B. s. coriacea* (Reeve, 1844). Given that this species has an extended planktonic larval stage, this finding was unexpected and raises questions as to what factors may have contributed to the divergence and isolation of populations in the Mediterranean and West Africa. However, the absence of genetic data from the Macaronesian part of the range hinders any discussion of this issue (Smriglio *et al.*, 2019). This data gap needs to be filled if the systematics and evolution of *B. scrobilator* are to be understood.

Here, we present the first geographically extensive molecular systematic study of *B. scrobilator*. Using an integrative taxonomic approach, our study is based on the phylogenetic analysis of DNA sequence data for the cytochrome *c* oxidase subunit I (COI) barcoding fragment and includes newly generated COI data for samples from Macaronesia and the Mediterranean. We used species delimitation methods to confirm if this expanded COI dataset supports Smriglio *et al.*'s (2019) hypothesis of two subspecies and to understand the relationship of the Macaronesian specimens to the Mediterranean and West African populations. Our expectation would be that, as a gastropod with a long-lived planktonic larval stage, *B. scrobilator* would show weak or no phylogeographic structure and little or no spatially structured variation in genetic and morphological characters. Thus, in describing the genetic diversity of *B. scrobilator*, we also evaluated if these two predictions are supported by currently available data.

MATERIAL AND METHODS

Samples

All the Macaronesian specimens of *Bursa scrobilator* used in this study were collected by scuba diving and subsequently fixed in 70–100% ethanol. Due to their extreme rarity in the wild, the Mediterranean specimens used in the study were found through careful searching of local museums and private collections; these samples consisted of two recently collected specimens (MED-PC-1, BAU-3539), which had been fixed in 70–100% ethanol, and three 'old' (historical) specimens, of which one was in denatured alcohol (MED-PC-3), one was an ethanol-preserved sample (MOL-052) from the Stazione Zoologica Anton Dohrn (SZN, Naples) and one was a dried sample (MED-PC-4; see Trillò, 2001). Sampled localities are summarized in Table 1 with voucher ID codes.

Radulae were extracted from dissected buccal masses after tissues had been partly dissolved in 10% sodium hydroxide, then rinsed in distilled water and observed under a stereo microscope. Selected radulae and protoconchs were air-dried, mounted on scanning electron microscope (SEM) stubs and gold–palladium-coated in a SC7640 sputter coater. They were then examined under a Jeol JSM-6700F SEM. Some of the more recently sampled specimens (e.g. SZN-MOL-0024, BAU-3536.2, BAU-3539) were dissected, and gross anatomy was examined under a stereo microscope. Our samples included one juvenile specimen (BAU-3535.3); the protoconch sculpture of this individual was fully intact, so it could be described in detail.

DNA extraction, amplification and sequencing

Samples from museums and those that had been preserved for an extended period were first transferred to fresh absolute ethanol for 1 week. A piece of tissue was dissected from the foot of each specimen, and DNA extraction was performed using a phenol-chloroform protocol after hydration and tissue digestion in proteinase K (see Oliverio & Mariottini, 2001). The 658-bp DNA barcode fragment of the mitochondrial COI gene was amplified using Folmer *et al.*'s (1994) universal primers, LCO1490 and HCO2198. PCR amplification conditions were as follows: initial denaturation at 95° C for 3 min; 35 cycles at 94° C for 30 s, 48° C for 30 s and 72° C for 60 s; and a final extension step of 72° C at 10 min. PCR products were purified with the Sigma-Aldrich GenElute Gel Extraction Kit following the manufacturer's instructions, and the amplicons were sequenced using the Folmer primers at the Molecular Biology and Sequencing Service of SZN, Naples.

Species delimitation and phylogenetic analyses

Sequences were retrieved from the GenBank and Barcode of Life Data System (BOLD) databases by searching for DNA barcodes of specimens belonging to the genus *Bursa*; the taxonomic identifications in the two databases were cross-checked with the most recent taxonomic literature on the family *Bursidae* (Castelin *et al.*, 2012; Sanders *et al.*, 2017; Smriglio *et al.*, 2019; Strong *et al.*, 2019). The ingroup consisted of 13 species of *Bursa*: *B. scrobilator*; *B. affinis* (Broderip, 1833); *B. awatii* Ray, 1949; *B. bufonia* (Gmelin, 1791); *B. cubaniana* (d'Orbigny, 1841); *B. elisabettae* Nappo, Pellegrini & Bonomolo, 2014; *B. fijiensis* (R. Watson, 1881); *B. fosteri* Beu, 1987; *B. granularis* (Röding, 1798); *B. larmacki* (Deshayes, 1853); *B. quirihorai* Beu, 1987; *B. rosa* (Perry, 1811); and *B. tuberosissima* (Reeve, 1844). The outgroup comprised *Tonna galea* (Linnaeus, 1758), *Ranella olearium* (Linnaeus, 1758) and *Galeodea echinophora* (Linnaeus, 1758), with trees rooted on *T. galea*. COI sequences were aligned manually; the alignments are available from the authors on request.

Species delimitation analyses were performed using an integrative taxonomic approach, where species are considered as hypotheses to be tested by independent evidence. Every sequenced specimen was identified to species level based on morphology, following which the COI barcode dataset (in-group only) was analysed using two methods, the distance-based automatic barcode gap discovery (ABGD) (Puillandre *et al.*, 2012) and the monophyly-based Bayesian Poisson tree process (bPTP) (Zhang *et al.*, 2013). The ABGD analysis was run on the online ABGD web server (http://wwwabi.snv.jussieu.fr/public/abgd/abgdweb.html) using the K2P substitution model, a relative gap width (X) of 1, a divergence of intraspecific diversity between 0.0001 and 0.1 and with Nb bins set at 20. The bPTP analysis was done using the bPTP web server (https://species.h-its.org); we ran the analysis for 200,000 Markov chain Monte Carlo (MCMC) generations with thinning set at 100 and burn-in at 0.1.

The software jModelTest 2 v. 0.1.7 (Darriba *et al.*, 2012) was used to select the best-fitting evolutionary model; model selection was based on the Akaike information criteria (Akaike, 1974), and the three codon positions of COI were analysed separately. Maximum likelihood (ML) analysis was performed using RAxML v. 0.6.0 (Kozlov *et al.*, 2019), with 1,000 bootstrap replicates (Felsenstein, 1985). Bayesian inference (BI) was performed using MrBayes v. 3.1.2 (Ronquist & Huelsenbeck, 2003). The MrBayes analysis involved two independent MCMC runs (with four chains per run) for 10 million generations, sampling every 100 generations. Branches were considered to be strongly (well) supported if bootstrap (BS) values $\geq$70 (Hillis & Bull, 1993) and Bayesian posterior probabilities (PP) $\geq$ 0.95 (Alfaro & Holder, 2006).

Spatial distribution of genetic diversity

Relationships between haplotypes were investigated using a median joining (MJ) approach (Bandelt *et al.*, 1999), as implemented in PopART (http://popart.otago.ac.nz; Leigh & Bryant, 2015). Phylogenetic network analyses may perform better than traditional tree-based phylogenetic methods when genetic divergence is low because they take into account population-level phenomena such as multifurcations and reticulations (Posada & Crandall, 2001). MJ, in particular, combines minimum spanning trees within a single network and adds median vectors (representing missing intermediates) to the network using a parsimony criterion.

Table 1. Localities of *Bursa scrobilator* sampled for this study, along with associated collection data, voucher numbers and GenBank accession numbers for COI sequences. All localities are in the East Atlantic–Mediterranean area and belong to the following regions: AZ, Azores Islands; CI, Canary Islands; M, Mediterranean Sea; WA, West Africa.

Region	Sampling locality, depth and collector	Coordinates (latitude, longitude)	Source	Voucher ID code	GenBank acc. no. for COI data
AZ	Fajã Grande, Flores Island, 12 m (leg. M.O., Aug. 2008)	39.4569, −31.2649	This study	BAU-3535.1	MN263830
AZ	Caloura, São Miguel Island, 8 m (leg. M.O., Sep. 2008)	37.70669, −25.508	This study	BAU-3536.1	-
AZ	Fajã Grande, Flores Island, 12 m (leg. M.O., Aug. 2008)	39.4569, −31.2649	This study	BAU-3535.2	MN263831
AZ	Fajã Grande, Flores Island, 12 m (leg. M.O., Aug. 2008)	39.4569, −31.2649	This study	BAU-3535.3	-
AZ	Caloura, São Miguel Island, 8 m (leg. M.O., Sep. 2008)	37.70669, −25.508	This study	BAU-3536.2	MN263832
CI	Las Eras, Tenerife Island, ∼20 m (leg. J.M. Barrios, Feb. 2010)	28.19796, −16.4194	This study	SZN-MOL-0021	MN263833
CI	Las Eras, Tenerife Island, ∼20 m (leg. J.M. Barrios, Feb. 2010)	28.19796, −16.4194	This study	SZN-MOL-0022	MN263834
CI	Las Eras, Tenerife Island, ∼20 m (leg. J.M. Barrios, Feb. 2010)	28.19796, −16.4194	This study	SZN-MOL-0023	MN263835
CI	Las Eras, Tenerife Island, ∼20 m (leg. J.M. Barrios, Feb. 2010)	28.19796, −16.4194	This study	SZN-MOL-0024	MN263836
CI	Las Eras, Tenerife Island, ∼20 m (leg. J.M. Barrios, Feb. 2010)	28.19796, −16.4194	This study	SZN-MOL-0025	MN263837
CI	Las Eras, Tenerife Island, ∼20 m (leg. J.M. Barrios, Feb. 2010)	28.19796, −16.4194	This study	SZN-MOL-0026	MN263838
CI	Punta de Teno, Tenerife Island, ∼11 m (leg. M.O., Jul. 1996)	28.34053, −16.9197	This study	BAU-3537	MN263839
CI	Puerto del Carmen, Lanzarote Island, ∼18 m (leg. M.O., Feb. 1995)	28.91814, −13.6693	This study	BAU-3538	MN263840
M	Reggio Calabria, Altafiumara, 5 m (leg. F.C, AV, W. Renda, Aug. 2009)	38.24446, 15.67524	This study	MED-PC-1	MN263841
M	Marettimo, Punta Bassana, 11 m (leg. M.O., Jul. 2011)	37.94907, 12.09144	This study	BAU-3539	MN263842
M	Messina, Pace, 5–7 m (leg. P. Micali, *c.* 1980)	38.23237, 15.57216	This study	MED-PC-3	MN263843
M	Naples (leg. C.P. Franceschini, May 1911)	40.81908, 14.22441	This study	MOL-052	MN263844
M	Ustica, 10 m (leg. P. Trillò, Aug. 1999)	38.71542, 13.15555	This study	MED-PC-4	-
M	Linosa Island, Italy	35.86805, 12.88163	Smriglio *et al.* (2019)	MOL-RM3.1	LS483261
M	Naples, Italy	40.63015, 14.36087	Smriglio *et al.* (2019)	MOL-RM3.2	LS483262
M	Blue Grotto, Malta	35.8208, 14.45682	Smriglio *et al.* (2019)	MOL-RM3.3	LS483263
WA	Dakar, Senegal	14.75057, −17.5274	Smriglio *et al.* (2019)	MNHN-IM-2009-11 908	LS483264
WA	Dakar, Senegal	14.75057, −17.5274	Smriglio *et al.* (2019)	MNHN-IM-2009-11 909	LS483265
WA	Dakar, Senegal	14.75057, −17.5274	Smriglio *et al.* (2019)	MNHN-IM-2009-11 911	LS483266

To investigate the spatial distribution of genetic diversity within each species, we carried out both an isolation by distance (IBD) analysis and a spatial principal component analysis (sPCA). IBD, as proposed by Wright (1940), is defined as a decrease in the genetic similarity among populations as the geographic distance between them increases. The presence of an IBD pattern can be detected by a nonparametric Mantel test, which is commonly used to test for nonrandom associations between a matrix of genetic distances and a matrix of geographical distances. The genetic distance matrix consisted of K2P pairwise intraspecific genetic distances for the COI alignment, which we computed using MEGA v. 6.0 (Tamura *et al.*, 2013). For the geographical distance matrix, we calculated the shortest marine distance between all pairs of collecting points using Google Earth v. 7.1.2.2041. Both matrices were used as input for IBDW v. 2.0 (Jensen *et al.*, 2005) and 30,000 randomizations. Despite the widespread use of Mantel tests to identify IBD patterns, theoretical reasons and the fact that these tests can be biased by spatial autocorrelation have led their reliability to be questioned (e.g. Meirmans, 2012). Therefore, to avoid misinterpretation of the potential correlations between genetic diversity and spatial distribution, we integrated the Mantel test with a sPCA, as implemented in the R package *adegenet* v. 2.1.0 (Jombart, 2008). This spatially explicit approach takes into account the genetic variance among studied samples, as well as their spatial autocorrelation (Jombart *et al.*, 2008). The detection of spatial features in the input data is carried out by incorporating Moran's I statistics (Moran, 1948, 1950) into the georeferenced genetic data. Moran's I ranges from -1 to $+1$, with values close to $+1.0$ indicating clustering and values close to -1.0 indicating dispersion. To define neighbours for calculation of Moran's I, a Gabriel graph for individual sample locations was

generated. Global and local tests based on 99,999 Monte Carlo permutations were used to interpret global and local components of the sPCA. The presence of significant global structuring may reflect patterns of spatial genetic structure (such as IBD), whereas significant local structuring may indicate strong differences between local neighbourhoods (repulsion) (Jombart *et al.*, 2008).

We calculated the number of haplotypes, nucleotide diversity (π) and haplotype diversity (HD). An analysis of molecular variance (AMOVA) was performed to compare intra- and inter-population genetic diversity when the specimens of *B. scrobilator* were grouped into three (Azores Islands, Canary Islands and Mediterranean) or two (Atlantic and Mediterranean) geographical clusters; a hierarchical analysis was performed, with statistical significance assessed by 1,000 permutations of the original data matrix followed by a Bonferroni adjustment (Rice, 1995). A mismatch analysis was also performed to estimate the most likely demographic dynamics of *B. scrobilator*; analyses were done using DnaSP v. 5.10 (Librado & Rozas, 2009) and Arlequin v. 3.5.1.3 (Excoffier *et al.*, 2005).

RESULTS

Morphology of Bursa scrobilator

No major differences were observed between the Macaronesian and Mediterranean specimens of *Bursa scrobilator*, and the description that follows applies to all examined specimens from the Canary Islands, the Azores and the Mediterranean.

Conchology

Shell thick and solid, moderately large for the genus (5–9 cm) (Fig. 1). Larval shell elongate-mammillate, light brown in colour, *c.* 2.5 in maximum diameter and consisting of 3.75 convex whorls (Fig. 2A–C); protoconch almost invariably corroded in adults, showing ~15% variation in size between different geographic areas, as well as among specimens within the same area. Protoconch I 0.5 whorl, with densely pitted sculpture ending in three to four axial riblets (Fig. 2D). Protoconch II 2.25 whorls, with cancellate sculpture of axial riblets and three spiral cordlets (Fig. 2E). Teleoconch five to six whorls, sculptured by four major spiral cords, usually knobbed; large varices sculptured with knobs at intersections with spirals. A few specimens devoid of obvious sculpture, with nodules just visible on penultimate varix and on peristome. Aperture large and columellar callus with 12 to 18 small folds. Colour of shell fawn, with whitish and reddish marbling and four reddish brown spiral lines overlapping the spiral cords. Light brown operculum (Fig. 1A), with anteriorly terminal nucleus (Fig. 1G, H).

Gross anatomy

Body massive, with irregular white, brown, yellow and blue patches and small yellowish-orange speckles (Fig. 1A). A pair of tentacles with small, dark and round eyes on swellings at their outer bases; tentacles marked with dark annular stripes and sparse yellow-orange speckles (Fig. 1A). Proboscis short and wide, pleurembolic, flattened elliptical and strongly muscularized; dark blue, with an electric-blue ring at tip (Fig. 1B). Jaw plates missing. Radula taenioglossate (formula 2.1.1.1.2; Fig. 3A–C), remarkably variable between and within individuals. Rachidian teeth broad, usually with long, slender and elongated median cusp and two shorter lateral cusps (Fig. 3D–I); median cusp with variable number of secondary basal denticles (from two to four, varying even in same tooth (Fig. 3D–H); lateral cusps with basal triangular processes interlocking with column of central teeth. Lateral tooth large and sickle-shaped, with broad base, one–two denticles on inner edge and two–five denticles on outer edge (Fig. 3J–K). Sickle-shaped marginal teeth, with one or two denticles on inner edge (Fig. 3M–O). One specimen with very large radular ribbon (nearly twice the size of other specimens examined, as is clear from scale bars in Figure 3), thick central rachidian tooth with no secondary denticles, thick lateral teeth with no inner denticles and thick lateral teeth lacking denticles on both inner and outer edges of radular ribbon along its entire length (Fig. 3I, L, P). Three accessory salivary glands present. Digestive tract consisting of solid foregut (forming a C-shaped structure) with terminal caecum, followed by short thin duct and muscular stomach (Fig. 1G, H) that was empty in all the samples examined; short intestine leading to the rectum, which opens into the right side of the mantle cavity. Mantle cavity with large ctenidium, small bipectinate osphradium and hypobranchial gland (Fig. 1G). Males with large, muscular, tongue-shaped penis, deeply wrinkled on dorsal side, just behind right cephalic tentacle (Fig. 1H); seminal groove closed; large testis (flattened and disk-shaped) compacted over posterior part of stomach, with long and convoluted vas deferens that runs mostly along the body's right side (Fig. 1H). Female gonad compacted in posterior part of the body, just over the muscular stomach (Fig. 1G); a small ovary with a swollen pallial oviduct was found in one apparently immature female (Fig. 1G).

Species delimitation for the genus Bursa and for Bursa scrobilator

Critical study of identifications for all COI sequences sourced from GenBank and BOLD revealed that, in several cases, sequences from the same specimens were assigned to different taxa in the two databases, with preliminary identifications having not been updated in GenBank/BOLD after publication of the relevant papers. Strong *et al.* (2019) have corrected almost all misidentifications or mismatches. Altogether, our data mining yielded COI sequences belonging to 13 bursid taxa (Tables 1 and 2). We generated COI sequence data for an additional 15 samples of *B. scrobilator* (Table 1). These samples comprised three individuals from the Azores, eight from the Canary Islands and four from the Mediterranean Sea. Whereas the new sequences were trimmed to 566 bp following their alignment with the GenBank sequences, sequence variation was analysed on the basis of the full-length (i.e. untrimmed) sequences.

The ABGD analysis yielded 13 putative species, which were largely congruent with the *a priori* morphology-based identifications of bursid species from across the world (Tables 1 and 2; Fig. 4). The bPTP analysis yielded 14 putative species, with *B. scrobilator* being split into two species; these two species, however, were not strongly supported (*B. s. scrobilator*: PP = 0.65; *B. s. coriacea*: PP = 0.71) (Fig. 4). With *B. quirihorai* and *B. fijiensis* treated as a single species, intraspecific genetic divergence for the bursid dataset, excluding *B. scrobilator*, ranged from 0 to 2.9% (Table 3); the minimum interspecific distance was 6.6%. When *B. quirihorai* and *B. fijiensis* were treated as distinct species (as in Castelin *et al.*, 2012), intraspecific genetic divergences ranged from 0 to 2.2%, and the minimum interspecific divergence was 2.9%. Both the bPTP analysis and the ABGD one showed the Mediterranean and Macaronesian sequences of *B. scrobilator* (altogether corresponding in morphology to the subspecies *B. s. scrobilator*) to belong to a single putative species. The very low K2P distances between specimens in the Mediterranean–Macaronesian clade (0–0.9%) (Fig. 4) agree with this finding. While the ABDG analysis showed the three Senegalese specimens (corresponding morphologically to the subspecies *B. s. coriacea*) to belong to the same species as the Mediterranean and Macaronesian specimens, in the bPTP analysis, they formed a distinct species (intragroup K2P divergence 0–0.5%). We note that genetic distances between the Senegalese specimens, on the one hand, and the Macaronesian–Mediterranean clade, on the other, were relatively high (1.6–2.7%).

Bayesian and ML phylogenies showed five well-supported clades, each comprising between one and four nominal species (Fig. 4). Clade I (PP = 0.99, BS = 80%) consisted of four species, *B. awatii*, *B. fosteri*, *B. quirihorai* and *B. fijiensis*, with strong support for the sister-group relationship of *B. awatii* and *B. fosteri* (PP = 0.99, BS = 83) and

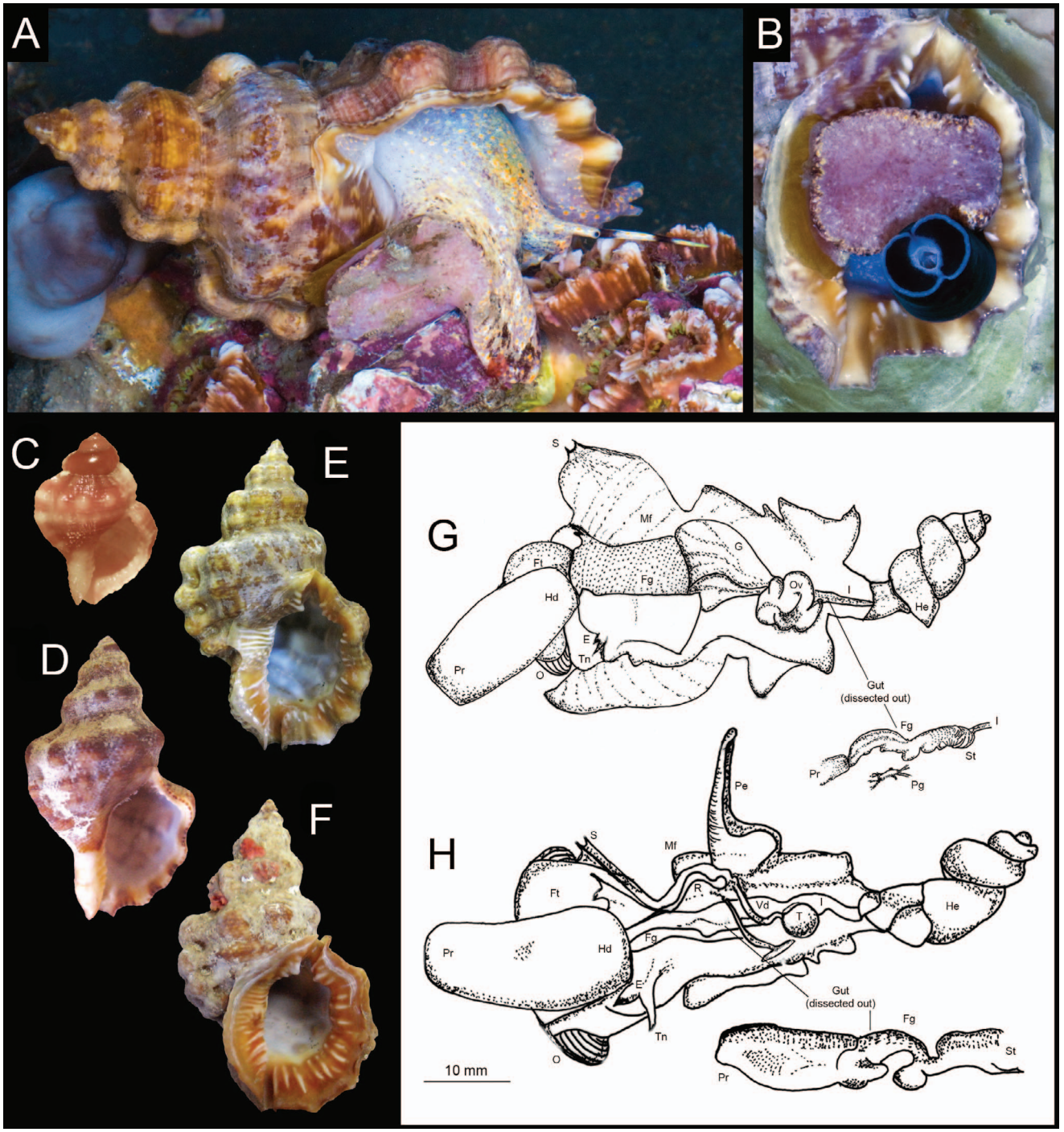

Figure 1. Shells and gross anatomy of *Bursa scrobilator*. **A.** Living individual from Altafiumara, Mediterranean (MED-PC-1). **B.** The same specimen with protruded proboscis. **C**–**F.** Representative specimens of different growth stages, as examined in this study. **C.** BAU-3535.3, Flores I., Azores, (shell height 0.9 cm). **D.** SZN-MOL-0026, Tenerife I., Canary Islands (shell height 3.2 cm). **E.** MED-PC-1, Altafiumara, Mediterranean (shell height 7 cm). **F.** SZN-MOL-0025, Tenerife I., Canary Islands (shell height 6.2 cm). **G**–**H.** Gross anatomy. **G.** SZN-MOL-0024, female (shell height 75 mm), with digestive tract removed along with the pedal ganglion. **H.** BAU-3539, male (shell height 79 mm), with digestive tract removed (see bottom right). Abbreviations: E, eye; Fg, foregut; Ft, foot; G, gill; Hd, head; He, digestive gland; I, intestine; Mf, mantle flap; O, operculum; Ov, ovary; Pe, penis; Pg, pedal ganglion; Pr, proboscis; R, rectum; S, inhalant siphon; St, stomach; T, testis; Tn, tentacle; and Vd, vas deferens.

of *B. quirihorai* and *B. fijiensis* (PP = 1, BS = 99%). Clade II, which was strongly supported only in the Bayesian analysis (PP = 0.96), also comprised four species, the relationships among which were unresolved. These were *B. lamarckii*, *B. rosa*, *B. tuberosissima* and *B. bufonia*. Clades III and IV were each composed of a pair of sister species; clade III was strongly supported only in the Bayesian analysis (PP = 0.98), whereas clade IV was strongly supported in both Bayesian and ML analyses (PP = 0.99, BS = 89%). Clade III consisted of the sister taxa *B. elisabettae* and *B. cubaniana* and clade IV comprised the sisters *B. granularis* and *B. affinis*. Clade V, *B. scrobilator*, was strongly supported (PP = 1, BS = 100%) and consisted of two strongly supported constituent clades corresponding to *B. s.*

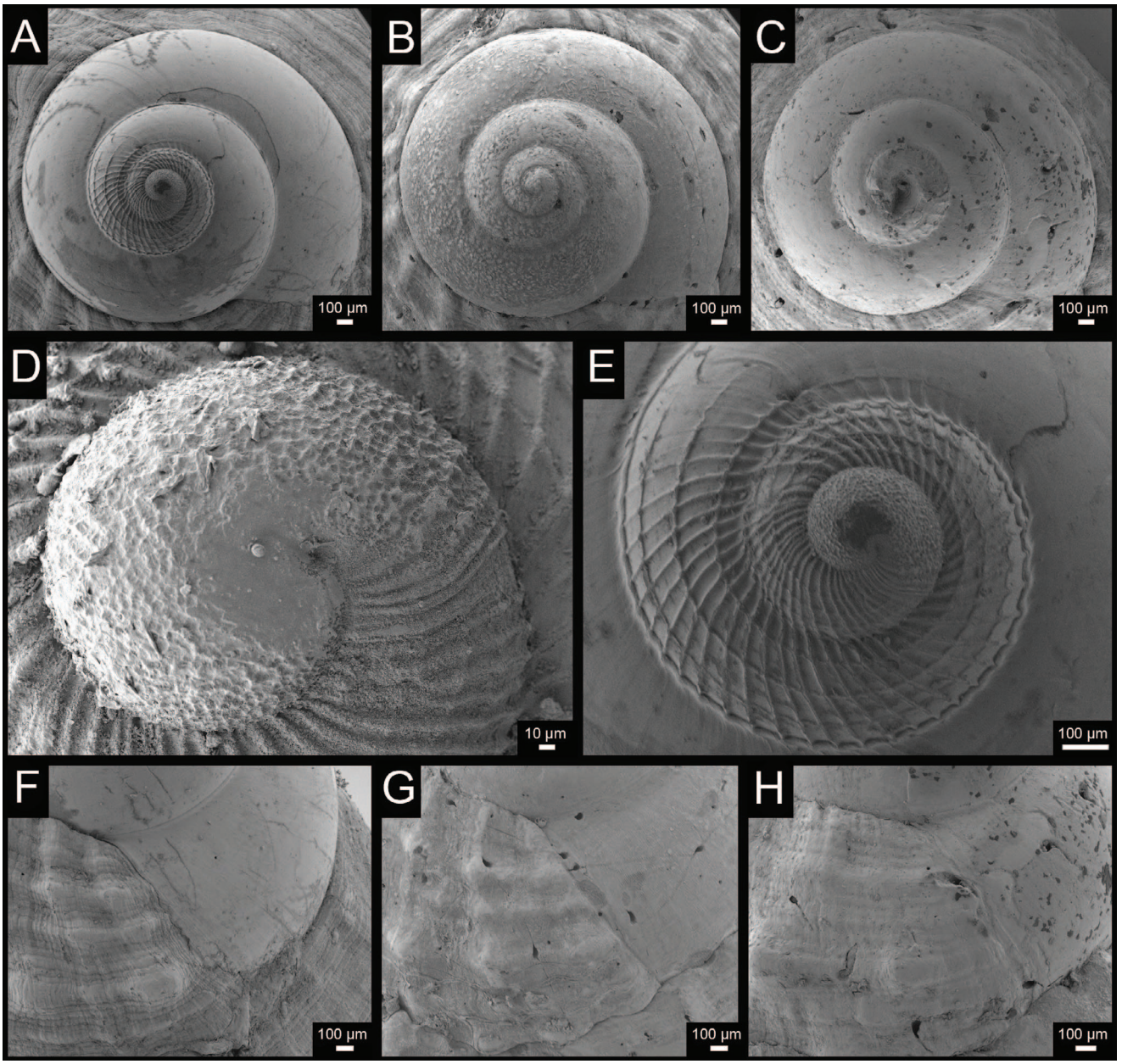

Figure 2. Features of the protoconch and early teleoconch of *Bursa scrobilator*. **A**–**C.** Protoconch. **A.** BAU-3535.3, Flores I., Azores. **B.** SZN-MOL-0026, Tenerife I., Canary Islands. **C.** MED-PC-1, Altafiumara, Mediterranean. **D.** Detail of protoconch I, BAU-3535.3, Flores I., Azores. **E.** Detail of protoconch II, BAU-3535.3, Flores I., Azores. **F**–**H.** Features of the early teleoconch. **F.** BAU-3535.3, Flores I., Azores. **G.** SZN-MOL-0026, Tenerife I., Canary Islands. **H.** MED-PC-1, Altafiumara, Mediterranean.

scrobilator (PP = 1, BS = 100%) and *B. s. coriacea* (PP = 1, BS = 100%), respectively. While the monophyly of 10 of the 13 species was strongly supported, intra-clade relationships were largely unresolved for those species represented by three or more specimens (Fig. 4). For the purposes of the present study, we treated the two constituent clades of *B. scrobilator* as separate subspecies, *B. s. scrobilator* and *B. s. coriacea* (but see the Discussion for further comments).

Phylogeographic structure and spatial distribution of genetic diversity in Bursa scrobilator

Nucleotide diversity was broadly similar at all locations, and haplotypic diversity was of the same magnitude at all hierarchical levels (Table 4). In the MJ network analysis, 17 polymorphic sites defined 11 haplotypes in *B. scrobilator*, with two major haploclades corresponding to the two ESUs *B. s. scrobilator* (eight haplotypes; π = 0.004) and *B. s. coriacea* (two haplotypes; π = 0.013) (Table 4; Fig. 5). Only the genetic diversity of the ESU corresponding to *B. s. scrobilator* was analysed; the ESU representing *B. s. coriacea* was represented by just three specimens from a single locality, so it could not be analysed. Nucleotide diversity was relatively low in *B. s. scrobilator*, with inter-population variance explaining only 2% of total variance (regardless of whether two or three geographical clusters were considered, both F-st and Φ-st were not significant). Mean intraspecific K2P distances for *B. scrobilator* were comparable to those of other bursids, but the maximum intraspecific K2P distance between *B. s. scrobilator* and *B. s. coriacea* was greater than the maximum intraspecific K2P distances estimated for the other species. The mismatch analysis, in which Macaronesian and

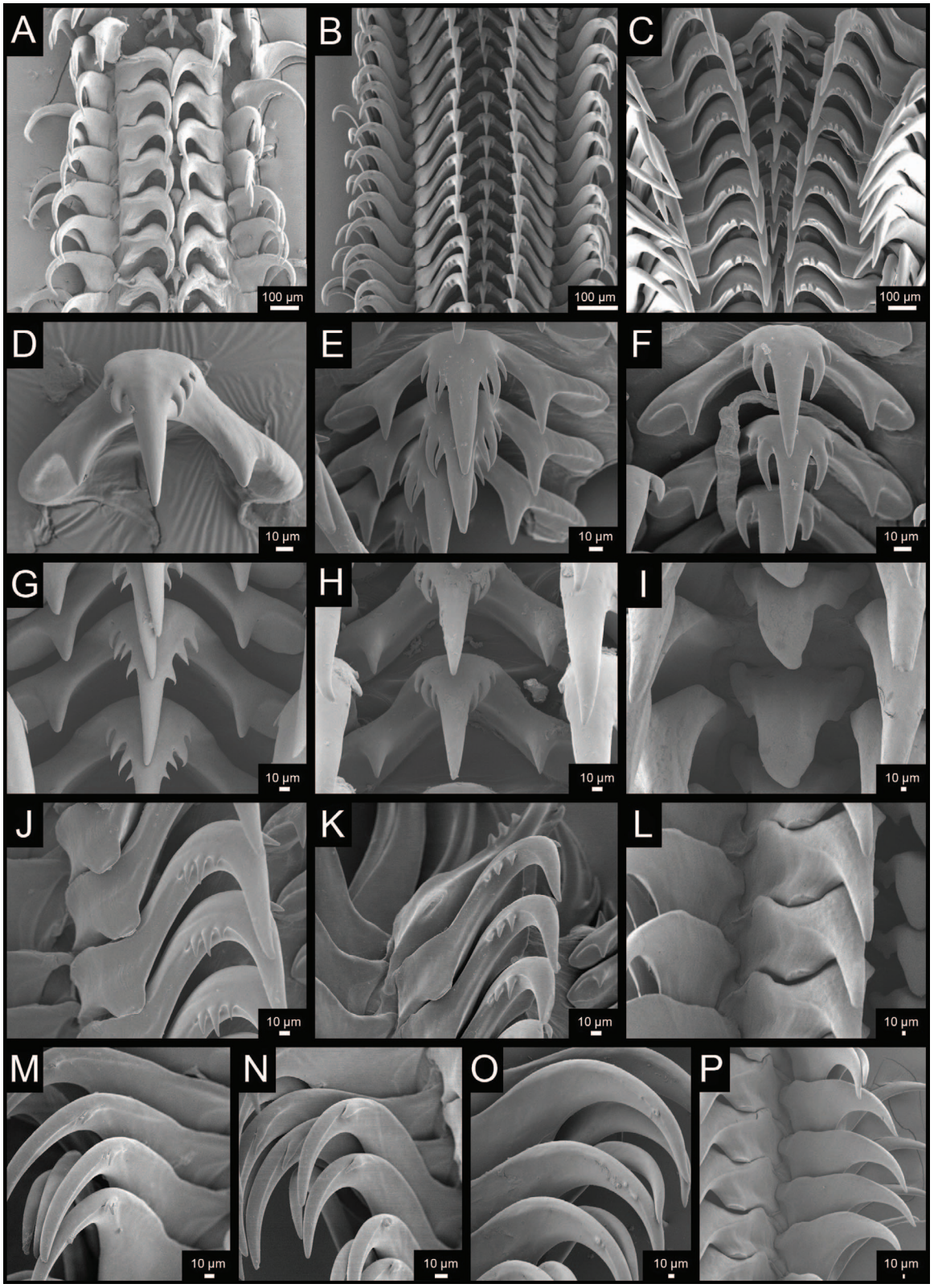

Figure 3. Features of the radula of *Bursa scrobilator*. **A**–**C.** Taenioglossate radula. **A.** BAU-3535.2, Flores I., Azores. **B.** SZN-MOL-0026, Tenerife I., Canary Islands. **C.** BAU-3539, Marettimo I., Mediterranean. **D**–**I.** Rachidian teeth. **D.** BAU-3535.2, Flores I., Azores. **E.** SZN-MOL-0025, Tenerife I., Canary Islands. **F.** SZN-MOL-0026, Tenerife I., Canary Islands. **G.** BAU-3539, Marettimo I., Mediterranean. **H.** MED-PC-3, Messina, Mediterranean. **I.** MED-PC-4, Ustica I., Mediterranean. **J**–**L.** Lateral teeth. **J.** SZN-MOL-0025, Tenerife I., Canary Islands. **K.** SZN-MOL-0026, Tenerife I., Canary Islands. **L.** MED-PC-4, Ustica I., Mediterranean. **M**–**O.** Marginal teeth. **M.** SZN-MOL-0025, Tenerife I., Canary Islands. **N.** SZN-MOL-0026, Tenerife I., Canary Islands. **O.** MED-PC-3, Marettimo I., Mediterranean. **P.** MED-PC-4, Ustica I., Mediterranean.

Table 2. GenBank and Barcode of Life Data System COI sequences used in the molecular systematic analyses and associated specimen data.

Species identifications				Voucher ID code	BOLD ID	GenBank acc. no. for COI	Locality (from databases or relevant paper/s)
This study	GenBank	As published in relevant molecular systematic study	Strong *et al.* (2019)				
Galeodea echinophora				MNHN-IM-2009-7834	TONO226-18	MH581337	France (Rungis International Market, Paris)
Ranella olearium				MNHN-IM-2007-36318	TONO231-18	MH581358	Mozambique Channel
Tonna galea				MNHN-IM-2013-56652	TONO278-18	MH581377	French Guiana
Tonna galea				MO77867	BIM225-13		Israel
B. affinis	*B. granularis*	*B. affinis* (2)	-	MNHN-IM-2013-11041	TONO128-17	MF124209	Papua New Guinea
B. affinis	*B. granularis*	*B. affinis* (2)	-	MNHN-IM-2013-52997	TONO145-17	MF124220	French Polynesia (Marquesas Islands)
B. affinis	*B. granularis*	*B. affinis* (1)	*B. affinis*	MNHN-IM-2007-43060	TONO098-12	JX241367	Vanuatu (Espiritu Santo Island)
B. affinis	*B. granularis*	*B. affinis* (2)	-	UF-422918	TONO157-17	MF124236	Micronesia (Kosrae Island)
B. affinis	*B. granularis*	*B. affinis* (2)	-	UF-423031	TONO158-17	MF124232	Marshall Islands (Eneko Channel, Majuro Atoll)
B. affinis	*B. granularis*	*B. affinis* (2)	-	UF-445316	TONO168-17	MF124189	Guam (Tepungan Channel, Piti)
B. affinis	*B. granularis*	*B. affinis* (2)	-	UF-445789	TONO169-17	MF124221	Japan (Okinawa Island, Okinawa Prefecture)
B. affinis	*B. granularis*	*B. affinis* (2)	-	UF-476657	TONO177-17	MF124218	New Caledonia (Huon Atoll)
B. affinis	*B. granularis*	*B. affinis* (2)	-	UF-493033	TONO179-17	MF124230	Philippines (Puerto Galera, Mindoro Province)
B. affinis	*B. granularis*	*B. affinis* (2)	-	UF-506838	TONO186-17	MF124214	Taiwan (Kenting National Park)
B. awatii	*B. awatii*	*B. awatii* (1)	-	MNHN-IM-2007-43 030	TONO066-12	JX241341	Solomon Islands (Gatokae Island)
B. awatii	*B. awatii*	*B. awatii* (1)	-	MNHN-IM-2007-43031	TONO030-12	JX241342	Philippines (Balicasag Island)
B. bufonia	*B. bufonia*	*B. bufonia* (1)	*B. tuberosissima*	MNHN-IM-2007-43041	TONO108-12	JX241350	Philippines (Panglao Island)
B. cubaniana	*B. granularis*	*B. cubaniana* (2)	*B. cubaniana*	MNHN-IM-2013-20 121	TONO129–17	MF124185	Guadeloupe (Malendure)
B. cubaniana	*B. granularis*	*B. cubaniana* (2)	-	UF-437625	TONO166-17	MF124241	Florida (Moneroe county)
B. elisabettae	*B. granularis*	*B. elisabettae* (2)	-	MNHN-IM-2009-23 312	TONO143-17	MF124238	Australia (Albany)
B. elisabettae	*B. granularis*	*B. elisabettae* (2)	-	MNHN-IM-2009-23 319	TONO144-17	MF124184	Australia (Albany)
B. fijiensis	*Bursina fijiensis*	*B. fijiensis* (1)	-	MNHN-IM-2009-5460	TONO089-12	JX241434	New Caledonia (north coast)
B. fijiensis	*Bursina fijiensis*	*B. fijiensis* (1)	*B. fijiensis*	MNHN-IM-2007-43 430	TONO013-12	JX241389	New Caledonia (south coast)
B. fijiensis	*Bursina fijiensis*	*B. fijiensis* (1)	-	MNHN-IM-2007-40 359	MSM105-08	JX241331	Australia (Lord Howe Island)
B. fijiensis	*Bursina fijiensis*	*B. fijiensis* (1)	-	MNHN-IM-2007-40 279	MSM025-08	JX241251	Australia (Norfolk Island)
B. fosteri	*B. fosteri*	*B. fosteri* (1)	*B. fosteri*	MNHN-IM-2007-43 048	TONO096-12	JX241356	Philippines (Bohol Island)
B. fosteri	*B. fosteri*	*B. fosteri* (1)	-	MNHN-IM-2009-22 032	TONO020-12	JX241423	New Caledonia
B. granularis	*B. granularis*	*B. granularis* (2)	-	MNHN-IM-2007-33115	TONO141-17	MF124186	Philippines (Panglao Island)
B. granularis	*B. granularis*	*B. granularis* (2)	-	MNHN-IM-2009-23292	TONO124-17	MF124212	Mozambique (Baie de Maputo, Inhaca Island)
B. granularis	*B. granularis*	*B. granularis* (2)	-	UF-423363	TONO160-17	MF124198	Madagascar (Hell-Ville, Nosy Be Island)
B. granularis	*B. granularis*	*B. granularis* (2)	-	UF-435487	TONO164-17	MF124222	Australia (Ningaloo Reef, Western Australia,)
B. granularis	*B. granularis*	*B. granularis* (2)	-	UF-476726	TONO178-17	MF124207	New Caledonia (Surprise Island)
B. granularis	*B. granularis*	*B. granularis* (2)	-	UF-445838	TONO170-17	MF124247	Japan (Okinawa)
B. granularis	*B. granularis*	*B. granularis* (2)	-	UF-506840	TONO188-17	MF124243	Saudi Arabia (Magna Coast Guard, Gulf of Aqaba)
B. granularis	*B. granularis*	*B. granularis* (1)	*B. granularis*	MNHN-IM-2007-43071	TONO019-12	JX241376	Vanuatu (Espiritu Santo Island)
B. lamarckii	*B. lamarckii*	*B. lamarckii* (1)	-	MNHN-IM-2007-43054	TONO008-12	JX241361	Vanuatu (Espiritu Santo Island)
B. lamarckii	*B. lamarckii*	*B. lamarckii* (1)	*B. lamarckii*	MNHN-IM-2007-43046	TONO112-12	JX241355	Philippines (Balicasag Island)
B. quirihorai	*B. quirihorai*	*B. quirihorai* (1)	-	MNHN-IM-2007-40259	MSM005-08	JX241231	Australia (Lord Howe Island)
B. quirihorai	*B. quirihorai*	*B. quirihorai* (1)	*B. quirihorai*	MNHN-IM-2007-43587	TONO002-12	JX241413	Australia (Norfolk Island)
B. quirihorai	*B. quirihorai*	*B. quirihorai* (1)	-	MNHN-IM-2007-40302	MSM048-08	JX241274	Australia (Norfolk Island)
B. rosa	*B. lamarckii*	*B. lamarckii* (1)	*B. rosa*	MNHN-IM-2007-43045	TONO099-12	JX241354	Vanuatu (Espiritu Santo Island)
B. tuberosissima	*B. lamarckii*	*B. lamarckii* (1)	*B. tuberosissima*	MNHN-IM-2007-43066	TONO113-12	JX241371	Philippines (Panglao Island)

Other than Strong *et al.* (2019), published identifications were obtained from Castelin *et al.* (2012) and Sanders *et al.* (2017), which are denoted by the numbers '1' and '2', respectively.

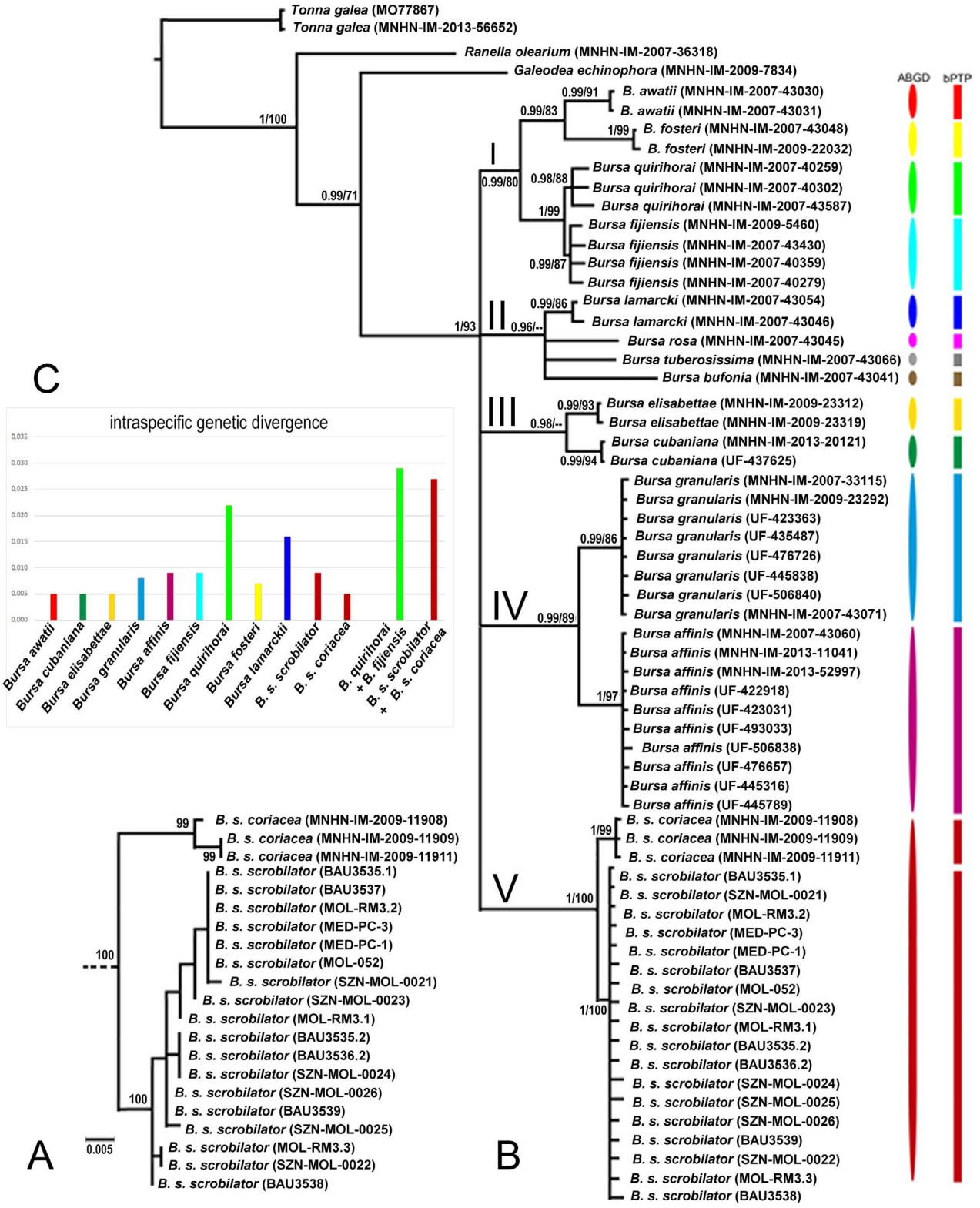

Figure 4. Phylogenetic relationships in the genus *Bursa*, based on COI sequence data. **A.** Part of ML tree showing relationships in the *Bursa scrobilator* clade (see clade V in B). **B.** Tree for the genus *Bursa* (the substitution models used for the first, second and third codon positions are TrN1+I+G, F81 and TPM3uf+G, respectively). Numbers along branches indicate Bayesian posterior probabilities and ML bootstrap values, respectively. Roman numerals I–V denote the five major clades. Putative species delimited by bPTP and ABGD methods are colour-coded. **C.** Histograms of the ranges of intraspecific genetic distances (K2P). *Bursa quirihorai* and *B. fijiensis* are considered first as separate ESUs and then as forming one ESU; *B. s. scrobilator* and *B. s. coriacea* are also shown in the same way.

Table 3. Range in intraspecific COI sequence divergence (% K2P) for species of *Bursa*.

Species	Minimum K2P	Maximum K2P	
Bursa awatii	0.000	0.005	
B. cubaniana		0.005	
B. elisabettae		0.005	
B. granularis	0.002	0.008	
B. affinis	0.000	0.009	
B. fijiensis	0.000	0.009	0.029*
B. quirihorai	0.000	0.022	
B. fosteri	0.000	0.007	
B. lamarckii	0.005	0.016	
B. scrobilator scrobilator	0.000	0.009	0.027**
B. scrobilator coriacea	0.000	0.005	

A single asterisk indicates the maximum value when *B. fijiensis* and *B. quirihorai* are a single ESU. Two asterisks denote the maximum value when *B. s. scrobilator* and *B. s. coriacea* are a single ESU.

Table 4. Nucleotide diversity (π) and haplotype diversity (HD) for the two ESUs of *Bursa scrobilator*, based on the COI alignment (*n* indicates the sample size).

ESU	Group	Subgroup	*n*	π	HD
B. s. scrobilator			18	0.004	0.853
	Atlantic		11	0.004	0.911
		Azores	3	0.004	0.667
		Canary I.	8	0.005	1.000
	Mediterranean	Mediterranean	7	0.003	0.714
B. s. coriacea	Senegal	Senegal	3	0.004	0.667

Mediterranean *B. s. scrobilator* were treated as one geographical cluster, showed a bimodal distribution (Fig. 6), suggesting demographic stability in recent times; regardless of whether analyses were based on two or three geographical clusters, the Tajima's *D* test was consistently not significant ($P > 0.10$). The *B. s. scrobilator* clade did not show any geographical structure, and constituent clades contained specimens from all sampled areas (Fig. 4). The Mantel test did not support any correlation between geographical and genetic distance ($0.142 \leq P \leq 0.493$). The sPCA showed that there was neither global ($P = 0.809$) nor local ($P = 0.115$) spatial structure in the genetic data (Fig. 7).

DISCUSSION

We found that for *Bursa scrobilator scrobilator* genetic connectivity over long distances (i.e. virtually across the whole range) was high, and we found no evidence of geographic structure at both local and global spatial scales. These results agree with what we would expect for a species with long-lived pelagic larvae. Our findings are also consistent with the little that is known on other species of *Bursa* (Castelin *et al.*, 2010) and with available data on other organisms with long-lived planktotrophic larvae (e.g. *Sassia remensa*, Castelin *et al.*, 2010; see also Staton & Rice, 1999). The pattern of genetic connectivity in *B. s. scrobilator* is relevant for several aspects of its biology; particularly important aspects in this respect are its taxonomic status and its capacity to respond to climate change.

As is common for most mollusc species, the taxonomy of *B. scrobilator* has long been focused solely on shell characters. Smriglio *et al.* (2019), in an in-depth morphological survey of Recent and fossil shells, published the first molecular systematic analysis for this species, showing that there was a deep genetic divergence between three Senegalese samples and three Mediterranean samples. This analysis formed part of a shell-based assessment of the taxonomic status of the West African morphotype (with finely granulose sculpture and fine to prominent shoulder nodules, corresponding to the nominal taxon *Ranella coriacea* Reeve, 1844) and the typical Mediterranean morphotype (corresponding to the nominal taxon *Murex scrobilator* Linnaeus, 1758). On the basis of the consistent, yet subtle shell morphological differences between Senegalese and Mediterranean samples (see also Cossignani, 1994; Ardovini & Cossignani, 2004; Beu, 2010), and supplementary genetic data, Smriglio *et al.* (2019) proposed two subspecies: *B. s. scrobilator* from the Mediterranean (probably including the Macaronesian populations) and *B. s. coriacea* (Reeve, 1844) from West Africa. By generating COI barcode data for specimens from the Azores and Canary Islands and for additional specimens from the Mediterranean region, we have substantially added to the genetic data available for this species. In our analyses, we found strong evidence for the Macaronesian and Mediterranean specimens forming a single clade and this clade being sister to a clade of exclusively Senegalese samples. This confirms the general morphological pattern first observed by Smriglio *et al.* (2019). For the purposes of the present study, we followed Smriglio *et al.* (2019) and treated the two constituent ESUs of *B. scrobilator* as distinct subspecies. However, we would argue that the status of the West African populations needs to be carefully assessed; their divergence from the Mediterranean–Macaronesian populations is relatively deep (1.6–2.7%, mean 2.1%) and comparable to the divergence between the sister species *B. quirihorai* and *B. fijiensis* (1.5–2.3%). Given their sympatric distribution and distinct ecology, Castelin *et al.* (2012) concluded that *B. quirihorai* and *B. fijiensis* were distinct species. In contrast, *B. s. scrobilator* and *B. s. coriacea* are allopatric, and this may justify their continued recognition as subspecies. *Bursa scrobilator* originated in the Proto-Mediterranean during the Middle Miocene (Sanders *et al.*, 2019). Smriglio *et al.* (2019) have speculated that the two extant subspecies of *B. scrobilator* may have diverged from each other between the end of the Miocene and the early Pliocene; that would be broadly similar to the molecular-clock-based minimum time of divergence (4.9 Myr; 95% probability interval of 2.5–7.5 Myr) estimated for *B. quirihorai* and *B. fijiensis* (Castelin *et al.*, 2012). However, as far as is currently known, the earliest confirmed records of *B. s. coriacea* are those figured by Beu (2010: pl. 7: figs 3, 4, 6, 7), and these are from the 'latest Pliocene–Early Pleistocene' of Costa Rica. This suggests a more recent split between the two ESUs (2–3 Myr), which would be consistent with ranking the two morphotypes as separate subspecies. We note that the genetic divergence between *B. s. scrobilator* and *B. s. coriacea* is roughly one third the minimum genetic distances observed between cryptic species in the *B. granularis* species complex (6.4%; Sanders *et al.*, 2017), which is a clade of at least four species, for which a maximum calibration age of 9 Myrs has been suggested (Sanders *et al.*, 2019). We suggest that a molecular phylogenetic study based on several loci and incorporating data from the recent review of fossil data by Sanders *et al.* (2019) should be carried out. This would allow the dating of the split between the two ESUs and would thus place future taxonomic assessments of *B. scrobilator* in a robust temporal framework. The relatively deep genetic divergence observed between the two subspecies parallels the taxonomic separation between Macaronesian and West African populations in other gastropods with planktotrophic larvae. For instance, *Columbella adansoni* from Macaronesia and *C. xiphitella* from West Africa, both of which have planktotrophic development, are distinct species (Russini *et al.*, 2017); *C. adansoni* is sister to the Mediterranean species *C. rustica* (with nonplanktotrophic development). The long-lived teleplanic larvae of *Bursa* may have hampered speciation, whereas the more typical (short-lived) planktotrophic larvae of the Atlantic *Columbella* may have allowed the divergence and subsequent speciation of West African and Macaronesian populations; speciation has involved the loss of planktotrophy in *C.*

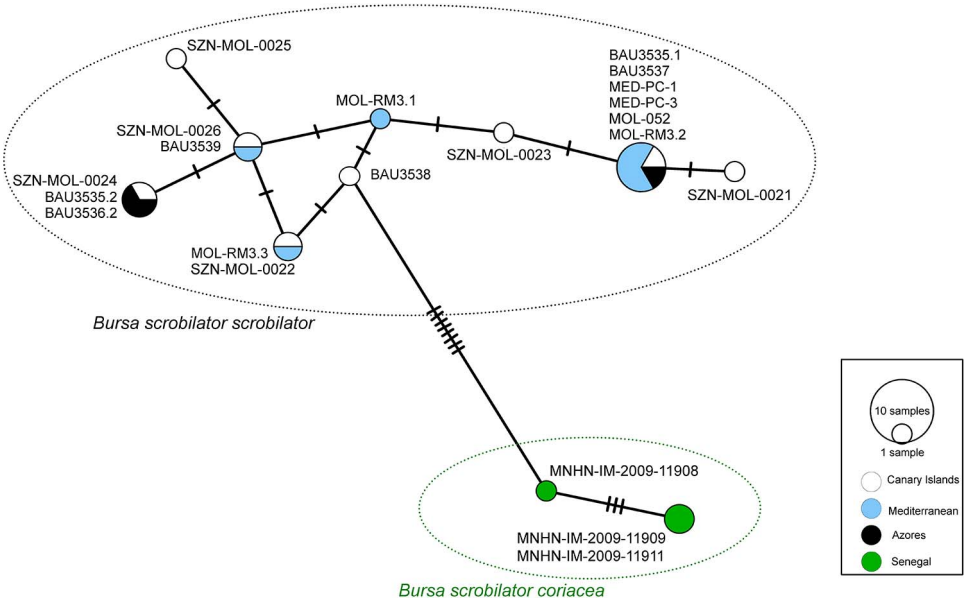

Figure 5. MJ network for the haplotypes of *Bursa scrobilator*. The length of the branches connecting the different haplotypes is proportional to the number of mutations. Small segments along the connecting branches represent missing intermediate haplotypes (identified using a parsimony criterion).

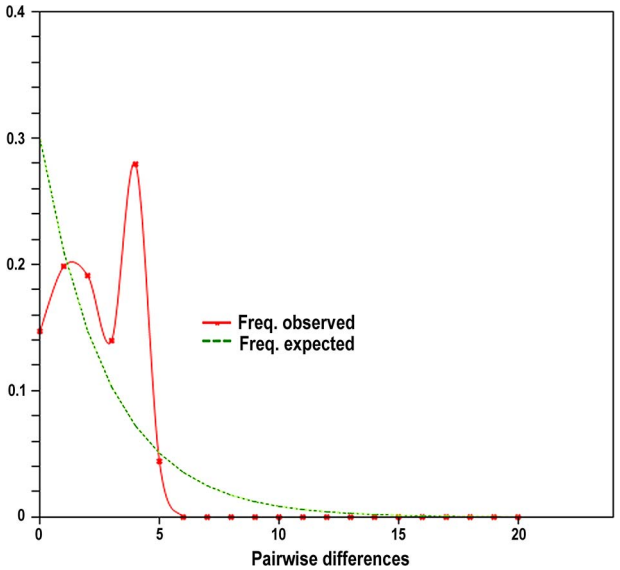

Figure 6. Mismatch distribution showing bimodal distribution.

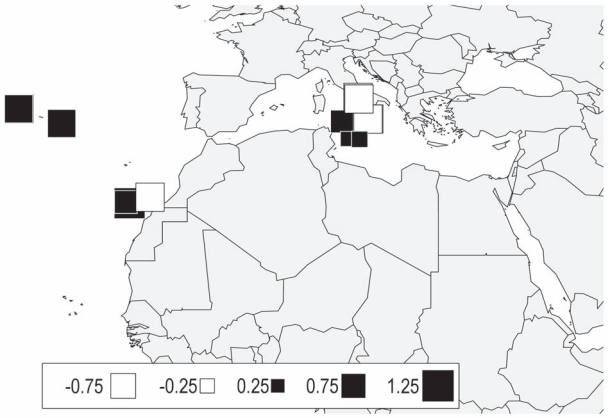

Figure 7. Spatial distribution of the scores of PC1 obtained from the sPCA for *Bursa scrobilator scrobilator*. Each square corresponds to a sampled locality with the colour of the square indicating the score of the relevant haplotype (positive if black, negative if white).

rustica when it diverged from *C. adansoni* at *c.* 2 Mya, as estimated by Oliverio (1995).

The gross anatomy of the Mediterranean–Macaronesian *B. s. scrobilator* agrees with the relatively scanty knowledge that we have of the family (Houbrick & Fretter, 1969; Beu, 1981). For their large dataset, Smriglio *et al.* (2019) observed substantial homogeneity in adult shell morphology, and that is paralleled here—albeit for a small number of samples—by homogeneity in other morphological characters (protoconch, radula and gross anatomy) across the entire range of *B. s. scrobilator*. The well-preserved protoconch observed in one of the juvenile shells studied by us (Fig. 2A, D–E) was reticulately sculptured; this character has not been observed so far, not even in the Pliocene specimen from Estepona (see Landau *et al.*, 2004), which our examinations show has a worn protoconch. The elusive nominal taxon *Talisman parfaiti* de Folin, 1887, the holotype of which we figure for the first time (Fig. 8; see also description by de Folin, 1884), was originally described on the basis of a bursid larval shell (Warén & Bouchet, 1990; Beu, 2010), which was collected from southwestern Europe or West Africa. Based on the strongly reticulate sculpture of protoconch II, we suggest that *Talisman parfaiti* was likely based on a larval shell of *B. scrobilator*.

We found strikingly high intra(sub)specific and intra-individual variation in radular characters, but there was no geographic basis to this variation. The variability in radular characters is also evident in a specimen described by Melone (1975); apart from the radula of MED-PC-4 (Fig. 3I, L, P), the radula described by Melone differs from all the other radulae examined by us. We can say little about the generality of this variability; only a few bursid radulae have been illustrated to date (Beu, 1981; Ekawa & Toki, 2005; Barkalova *et al.*, 2016), and no published data are available for the family on the intraspecific variation in radular characters. It may be that the *Bursidae* show plasticity in radular characters. Ontogenetic change and sexual dimorphism are known to be potential modulators of radular

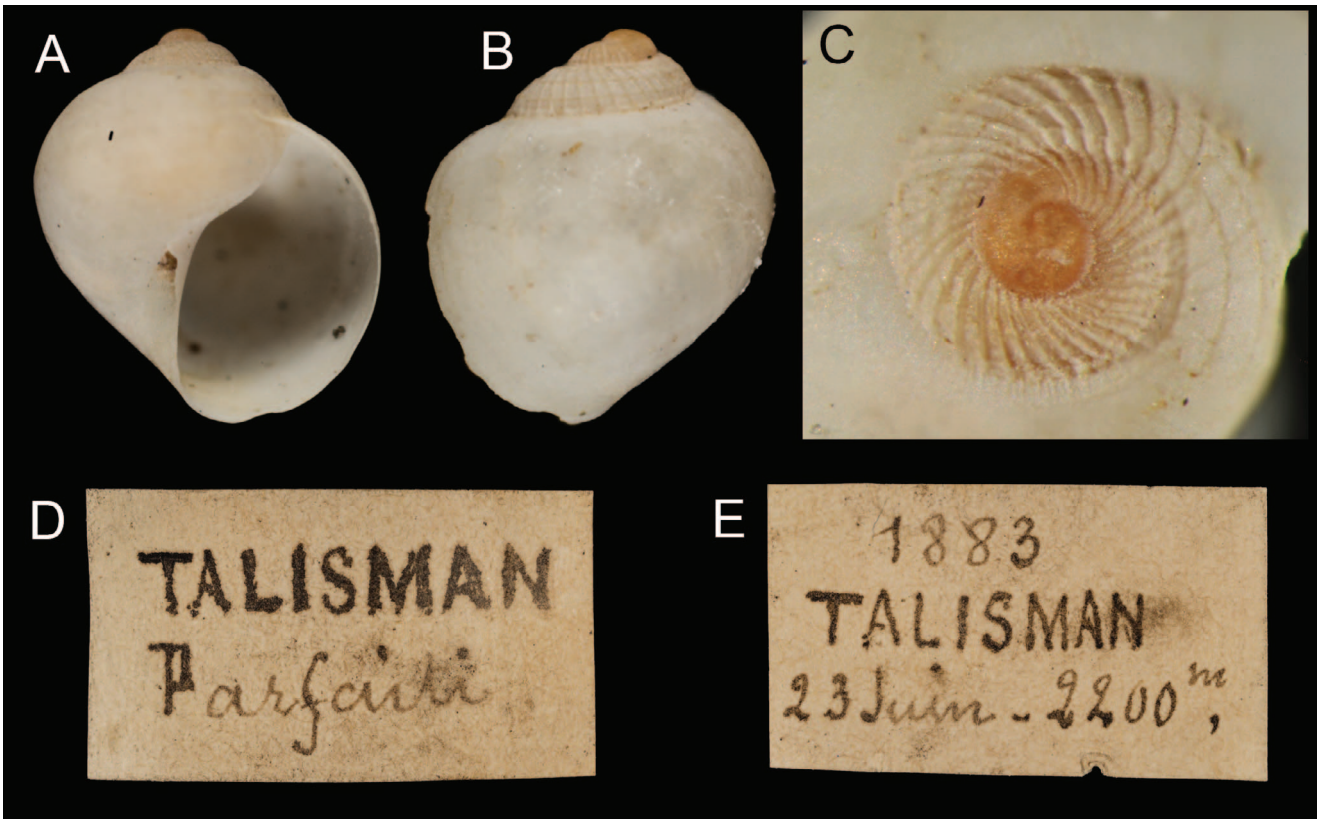

Figure 8. Holotype of *Talisman parfaiti* from the Travailleur and Talisman collection, Muséum national d'Histoire naturelle, Paris (shell height 1.5 mm). **A**–**C.** Apertural (**A**), dorsal (**B**) and apical (**C**) views of the shell. **D**–**E.** Original labels.

features in molluscs (e.g. Maes, 1966; Bertsch, 1976; Nybakken & Perron, 1988; Meirelles & Matthews-Cascon, 2003; Mutlu, 2004; Matthews-Cascon *et al.*, 2005; Warén, 2005; Martínez-Pita *et al.*, 2006). However, the variation we observed was not related to sex (discriminated on the basis of the presence/absence of the penis) or age (evaluated on the basis of total shell height). Our observations are paralleled by those of Barkalova *et al.* (2016), who reported two very different types of radula from two species of the bursid genus *Tutufa* Jousseaume, 1881. Whereas the radula of *Tutufa oyamai* was very similar to the typical radula of *Bursa* (this applies also to all but one of the radulae examined in our study), that of *Tutufa rubeta* was extremely fatty and similar to the radula of *B. scrobilator* figured by Melone (1975) and to just one of our specimens (MED-PC-4). No explanation, however, was offered by Barkalova *et al.* (2016) for the differences they observed.

Caution is needed when discussing the results of population genetics and morphological analyses based on small sample sizes. This is especially the case when assessing the effects of patterns of genetic connectivity—likely to be complex in the case of long-lived pelagic larvae—on mutation-drift equilibria (Flowers *et al.*, 2002). The mismatch distribution suggests that the demography of the nominal subspecies of *B. scrobilator* has been relatively stable in recent times. This is interesting because *B. scrobilator* has long been considered to be a rare species in the Mediterranean. However, several anecdotal reports from amateur collectors and marine biologists in the last few years seem to indicate an increase in the number of records from Mediterranean sites. If this increase is confirmed in the future, then it suggests the hypothesis that rising temperatures and, more generally, climate change, which are favouring thermophilic species in the Mediterranean Sea (e.g. Moullec *et al.*, 2016 and references therein), may also affect the distribution and population biology of *B. scrobilator*.

ACKNOWLEDGEMENTS

We would like to thank Javier Martin Barrios (Spain), Pasquale Micali (Italy) and Piergiorgio Trillò (Italy), who generously contributed material from their private collections. Flegra Bentivegna (Italy) and Andrea Travaglini (Italy) gave us access to preserved material deposited in SZN. Our colleagues Giovanni Fulvio Russo (Italy), Paolo Sordino (Italy), Francesco Toscano (Italy) and Valerio Zupo (Italy) provided useful insights. Manuel Caballer Gutiérrez (Spain) and Virginie Héros (France) provided the photos of *Talisman parfaiti*. Finally, we would like to thank the two anonymous reviewers who provided constructive and helpful feedback on the manuscript and Dinarzarde Raheem for extensive editorial input.

REFERENCES

AKAIKE, H. 1974. A new look at the statistical model identification. *IEEE Transactions on Automatic Control*, **19**: 716–723.

ALFARO, M.E., & HOLDER M.T. 2006. The posterior and the prior in Bayesian phylogenetics. *Annual Review of Ecology Evolution and Systematics*, **37**: 19–42.

ARDOVINI, R. & COSSIGNANI, T. 2004. *West African seashells*. L'Informatore Piceno, Ancona.

AYRE, D.J., MINCHINTON, T.E. & PERRIN, C. 2009. Does life history predict past and current connectivity for rocky intertidal invertebrates across a marine biogeographic barrier? *Molecular Ecology*, **18**: 1887–1903.

BANDELT, H.J., FORSTER, P. & RÖHL, A. 1999. Median-joining networks for inferring intraspecific phylogenies. *Molecular Biology and Evolution*, **16**: 37–48.

BARKALOVA, V.O., FEDOSOV, A.E. & KANTOR, Y.I. 2016. Morphology of the anterior digestive system of tonnoideans (Gastropoda:

Caenogastropoda) with an emphasis on the foregut glands. *Molluscan Research*, **36**: 54–73.

BERTSCH, H. 1976. Intraspecific and ontogenetic radular variation in opisthobranch systematics (Mollusca: Gastropoda). *Systematic Biology*, **25**: 117–122.

BEU, A.G. 1981. Australian gastropods of the family Bursidae. Part 1. The families of Tonnacea, the genera of Bursidae, and revision of species previously assigned to *Tutufa* Jousseaume, 1881. *Records of the Australian Museum*, **33**: 248–324.

BEU, A.G. 1997. Superfamily Tonnoidea. In: *Mollusca: the southern synthesis. Fauna of Australia. Vol. 5: Part B* (P.L. Beesley, G.J.B. Ross & A. Wells, eds), pp. 792–803. CSIRO Publishing, Collingwood.

BEU, A.G. 1998. Indo-West Pacific Ranellidae, Bursidae and Personidae (Mollusca: Gastropoda). A monograph of the New Caledonian fauna and revisions of related taxa. Résultats des campagnes MUSORSTOM 19. *Mémoires du Muséum National d'Histoire Naturelle*, **178**: 1–255.

BEU, A.G. 2010. Neogene tonnoidean gastropods of tropical and south America: contributions to the Dominican Republic and Panama paleontology projects and uplift of the central American isthmus. *Bulletins of American Paleontology*, **377–378**: 1–550.

CASTELIN, M., LAMBOURDIERE, J., BOISSELIER, M.-C., LOZOUET, P., COULOUX, A., CRUAUD, C. & SAMADI, S. 2010. Hidden diversity and endemism on seamounts: focus on poorly dispersive neogastropods. *Biological Journal of the Linnean Society*, **100**: 420–438.

CASTELIN, M., LORION, J., BRISSET, J., CRUAUD, C., MAESTRATI, P., UTGE, J. & SAMADI, S. 2012. Speciation patterns in gastropods with long-lived larvae from deep-sea seamounts. *Molecular Ecology*, **21**: 4828–4853.

COSSIGNANI, T. 1994. *Bursidae of the world*. L'Informatore Piceno, Ancona.

COWEN, R.K. & SPONAUGLE, S. 2009. Larval dispersal and marine population connectivity. *Annual Review of Marine Science*, **1**: 443–466.

DARRIBA, D., TABOADA, G.L., DOALLO, R. & POSADA, D. 2012. JModelTest 2: more models, new heuristics and parallel computing. *Nature Methods*, **9**: 722.

DE FOLIN, L. 1884. Une série de mollusques des explorations de 1881–1883. *Les Fonds de la Mer*, **4**: 201–212.

EDMANDS, S. 2001. Phylogeography of the intertidal copepod *Tigriopus californicus* reveals substantially reduced population differentiation at northern latitudes. *Molecular Ecology*, **10**: 1743–1750.

EKAWA, K. & TOKI, Y. 2005. Notes on radulae of the family Bursidae (Gastropoda) from Kii Channel, Wakayama Prefecture, Japan. *Nanki Seibutsu*, **47**: 63–66. In Japanese.

ELLINGSON, R.A. & KRUG, P.J. 2016. Reduced genetic diversity and increased reproductive isolation follow population-level loss of larval dispersal in a marine gastropod. *Evolution*, **70**: 18–37.

EXCOFFIER, L., LAVAL, G. & SCHNEIDER, S. 2005. Arlequin 3.01: an integrated software package for population genetics data analysis. *Evolutionary Bioinformatics Online*, **1**: 47–50.

FELSENSTEIN, J. 1985. Confidence limits on phylogenies: an approach using the bootstrap. *Evolution*, **39**: 783–791.

FLOWERS, J.M., SCHROETER, S.C. & BURTON, R.S. 2002. The recruitment sweepstakes has many winners: genetic evidence from the sea urchin *Strongylocentrotus purpuratus*. *Evolution*, **56**: 1445–1453.

FOLMER, O., BLACK, M., HOEH, W., LUTZ, R. & VRIJENHOEK, R. 1994. DNA primers for amplification of mitochondrial cytochrome c oxidase subunit I from diverse metazoan invertebrates. *Molecular Marine Biology and Biotechnology*, **3**: 294–299.

HILLIS, D. & BULL, J.J. 1993. An empirical test of bootstrapping as a method for assessing confidence in phylogenetic analysis. *Systematic Biology*, **42**: 182–192.

HOUBRICK, H.S. & FRETTER, V. 1969. Some aspects of the functional anatomy and biology of *Cymatium* and *Bursa*. *Proceedings of the Malacological Society of London*, **38**: 415–429.

JABLONSKI, D. & LUTZ, R.A. 1983. Larval ecology of marine benthic invertebrates: paleobiological implications. *Biological Reviews*, **58**: 21–89.

JENSEN, J.L., BOHONAK, A.J. & KELLEY, S.T. 2005. Isolation by distance, web service. *BMC Genetics*, **6**: 13–18.

JOMBART, T. 2008. Adegenet: a R package for the multivariate analysis of genetic markers. *Bioinformatics*, **24**: 1403–1405.

JOMBART, T., DEVILLARD, S., DUFOUR, A.B. & PONTIER, D. 2008. Revealing cryptic spatial patterns in genetic variability by a new multivariate method. *Heredity*, **101**: 92–103.

KNOWLTON, N. & JACKSON, J.B. 1993. Inbreeding and outbreeding in marine invertebrates. In: *The natural history of inbreeding and outbreeding*. (N.W. Thornhill, ed.), pp. 200–249. University of Chicago Press, Chicago.

KOZLOV, A.M., DARRIBA, D., FLOURI, T., MOREL, B. & STAMATAKIS, A. 2019. RAxML-NG: a fast, scalable and user-friendly tool for maximum likelihood phylogenetic inference. *Bioinformatics*. doi: https://doi.org/10.1093/bioinformatics/btz305.

LANDAU, B., BEU, A. & MARQUET, R. 2004. The early Pliocene Gastropoda (Mollusca) of Estepona, Southern Spain—Part 5: Tonnoidea, Ficoidea. *Palaeontos*, **5**: 35–102.

LIBRADO, P. & ROSAS, J. 2009. DNASP v5: a software for comprehensive analysis of DNA polymorphism data. *Bioinformatics*, **25**: 1451–1452.

LIMA, G.M. & LUTZ, R.A. 1990. The relationship of larval shell morphology to mode of development in marine prosobranch gastropods. *Journal of the Marine Biological Association of the United Kingdom*, **70**: 611–637.

LEIGH, J.W. & BRYANT, D. 2015. PopART: full-feature software for haplotype network construction. *Methods in Ecology and Evolution*, **6**: 1110–1116.

LOWE, W.H. & ALLENDORF, F.W. 2010. What can genetics tell us about population connectivity? *Molecular Ecology*, **19**: 3038–3051.

MAES, V.O. 1966. Sexual dimorphism in the radula of the muricid genus *Nassa*. *Nautilus*, **79**: 73–80.

MARKO, P.B. 2004. 'What's larvae got to do with it?' Disparate patterns of postglacial population structure in two benthic marine gastropods with identical dispersal potential. *Molecular Ecology*, **13**: 597–611.

MARTÍNEZ-PITA, I., GUERRA-GARCÍA, J.M., SÁNCHEZ-ESPANA, A.I. & GARCÍA, F.J. 2006. Observations on the ontogenetic and intraspecific changes in the radula of *Polycera aurantiomarginata* García and Bobo, 1984 (Gastropoda: Opisthobranchia) from Southern Spain. *Scientia Marina*, **70**: 227–234.

MATTHEWS-CASCON, H.R., PEREIRA ALENCAR, H.A., GUIMARÂES RABAY, S. & MOTA, R.M.S. 2005. Sexual dimorphism in the radula of *Pisania pusio* (Linnaeus, 1758) (Mollusca, Gastropoda, Buccinidae). *Thalassas*, **21**: 29–33.

MAWDSLEY, J.R., O'MALLEY, R. & OJIMA, D.S. 2009. A review of climate-change adaptation strategies for wildlife management and biodiversity conservation. *Conservation Biology*, **23**: 1080–1089.

MEIRELLES, C.A.O. & MATTHEWS-CASCON, H. 2003. Relations between shell size and radula size in marine prosobranchs (Mollusca: Gastropoda). *Thalassas*, **19**: 45–53.

MEIRMANS, P.G. 2012. The trouble with isolation by distance. *Molecular Ecology*, **21**: 2839–2846.

MELONE, G. 1975. La radula di *Bursa scrobiculator* L. *Conchiglie*, **9–10**: 203–204.

MODICA, M.V., RUSSINI, V., FASSIO, G. & OLIVERIO, M. 2017. Do larval types affect genetic connectivity at sea? Testing hypothesis in two sibling marine gastropods with contrasting larval development. *Marine Environmental Research*, **127**: 92–101.

MORAN, P.A.P. 1948. The interpretation of statistical maps. *Journal of the Royal Statistical Society Series B*, **10**: 243–251.

MORAN, P.A.P. 1950. Notes on continuous stochastic phenomena. *Biometrika*, **37**: 17–23.

MOULLEC, F., BEN RAIS LASRAM, F., COLL, M., GUILHAUMON, F., HALOUANI, G., HATTAB, T., LE LOC'H, F. & YUNNE-JAI SHIN, Y.-J. 2016. Climate change impacts on marine resources. From individual to ecosystem responses. In: *The Mediterranean region under climate change* (J.-P. Moatti & S. Thièbault, eds), pp. 229–248. IRD Éditions, Marseille.

MUTLU, E. 2004. Sexual dimorphisms in radula of *Conomurex persicus* (Gastropoda: Strombidae) in the Mediterranean Sea. *Marine Biology*, **145**: 693–698.

NYBAKKEN, J. & PERRON, F. 1988. Ontogenetic change in the radula of *Conus magus* (Gastropoda). *Marine Biology*, **98**: 239–242.

OLIVERIO, M. & MARIOTTINI, P. 2001. A molecular framework for the phylogeny of *Coralliophila* and related muricoids. *Journal of Molluscan Studies*, **67**: 215–224.

OLIVERIO, M. 1995. Larval development and allozyme variation in the East Atlantic. *Columbella Scientia Marina*, **59**: 77–86.

POSADA, D. & CRANDALL, K.A. 2001. Intraspecific gene genealogies: trees grafting into networks. *Trends in Ecology and Evolution*, **16**: 37–45.

PUILLANDRE, N., LAMBERT, A., BROUILLET, S. & ACHAZ, G. 2012. ABGD, automatic barcode gap discovery for primary species delimitation. *Molecular Ecology*, **21**: 1864–1877.

RICE, J.A. 1995. Mathematical statistics and data analysis. Edn 2. Duxburry Press, Belmont, CA.

RONQUIST, F. & HUELSENBECK, J.P. 2003. MrBayes 3: Bayesian phylogenetic inference under mixed models. *Bioinformatics*, **19**: 1572–1574.

RUSSINI, V., FASSIO, G., MODICA, M.V., DEMAINTENON, M.J. & OLIVERIO, M. 2017. An assessment of the genus *Columbella* Lamarck, 1799 (Gastropoda: Columbellidae) from eastern Atlantic. *Zoosystema*, **39**: 197–212.

SANDERS, M.T., MERLE, D. & PUILLANDRE, N. 2019. A review of fossil Bursidae and their use for phylogeny calibration. *Geodiversitas*, **41**: 247–265.

SANDERS, M.T., MERLE, D., BOUCHET, P., CASTELIN, M., BEU, A.G., SAMADI, S. & PUILLANDRE, N. 2017. One for each ocean: revision of the *Bursa granularis* (Röding, 1798) species complex (Gastropoda: Tonnoidea: Bursidae). *Journal of Molluscan Studies*, **83**: 384–398.

SHANKS, A.L. 2009. Pelagic larval duration and dispersal distance revisited. *Biological Bulletin*, **216**: 373–385.

SMRIGLIO, C., FURFARO, G., TRILLÒ, P., APPOLLONI, M. & MARIOTTINI, P. 2019. A review of the Atlantic–Mediterranean *Bursa scrobilator* (Linnaeus, 1758) species complex. *Molluscan Research*. doi: https://doi.org/10.1080/13235818.2019.1600397.

STRATHMANN, M.F. & STRATHMANN, R.R. 2007. An extraordinarily long larval duration of 4.5 years from hatching to metamorphosis for teleplanic veligers of *Fusitriton oregonensis*. *Biological Bulletin*, **213**: 152–159.

STRONG, E.E., PUILLANDRE, N., BEU, A.G., CASTELIN, M. & BOUCHET, P. 2019. Frogs and tuns and tritons—a molecular phylogeny and revised family classification of the predatory gastropod superfamily Tonnoidea. *Molecular Phylogenetics and Evolution*, **130**: 18–34.

STATON, J.L. & RICE, M.E. 1999. Genetic differentiation despite teleplanic larval dispersal: allozyme variation in sipunculans of the *Apionsoma misakianum* species-complex. *Bulletin of Marine Science*, **65**: 467–480.

TAMURA, K., STECHER, G., PETERSON, D., FILIPSLI, A. & KUMAR, S. 2013. MEGA6: molecular evolutionary genetics analysis version 6.0. *Molecular Biology and Evolution*, **30**: 2725–2729.

THORSON, G. 1950. Reproductive and larval ecology of marine bottom invertebrates. *Biological reviews of the Cambridge Philosophical Society*, **25**: 1–45.

TRILLÒ, P. 2001. Prima segnalazione di *Cancelleria similis* Sowerby, 1833 e *Bursa scrobilator* Linnè, 1758 in Sicilia. *La Conchiglia*, **33**: 57–58.

WARÉN, A. & BOUCHET, P. 1990. Laubierinidae and Pisanianurinae (Ranellidae), two new deep-sea taxa of the Tonnoidea (Gastropoda: Prosobranchia). *Veliger*, **33**: 56–102.

WARÉN, A. 2005. Ontogenetic changes in the trochoidean (Archaeogastropoda) radula, with some phylogenetic interpretations. *Zoologica Scripta*, **19**: 179–187.

WRIGHT, S. 1940. Breeding structure of populations in relation to speciation. *American Naturalist*, **74**: 232–248.

ZHANG, J., KAPLI, P., PAVLIDIS, P. & STAMATAKIS, A. 2013. A general species delimitation method with applications to phylogenetic placements. *Bioinformatics*, **29**: 2869–2876.